Environmental Earth Sciences (2018) 77:115
https://doi.org/10.1007/s12665-018-7311-z

ORIGINAL ARTICLE

Pronounced changes in air quality, atmospheric and meteorological parameters, and strong mixing of smoke associated with a dust event over Bakersfield, California

Akshansha Chauhan[1] · Samara C. de Azevedo[2,3] · Ramesh P. Singh[2]

Received: 1 October 2017 / Accepted: 29 January 2018 / Published online: 8 February 2018

Abstract
On September 28, 2016, an intense dust storm impacted the city of Bakersfield and surrounding areas in California. The dust event coincided with smoke aerosols from the forest fire located in the northwest of Bakersfield. In California, forest fires are frequent during summer and fall seasons. The forest fire smoke plumes were subjected to large dispersion and appeared widespread. In this study, we present a detailed analysis of satellite and surface observations indicating pronounced changes in air quality, aerosol characteristics, trace gases, along the prevailing meteorological conditions over Bakersfield associated with the dust event and its interactions with the forest fire smoke. Back trajectory simulations clearly show inflow of the dust airmass from the Mojave Desert located east of Bakersfield, in contrast to the forward trajectories originating from the forest fire event located in the northwestern region, suggesting possibility of mixing of smoke and dust in the Bakersfield area. In addition, low and strong wavelength dependence of aerosol single scattering albedo also supports the observations of strong aerosol mixing of dust and smoke.

Keywords MODIS · AIRS · AQI · Dust · Aerosols · Forest fire · Satellite data · AERONET

Introduction

Dust storms are common throughout the globe, during spring and summer seasons. Long-range transport of dust mainly originates over desert regions where prevailing meteorological conditions affect the dust transport pathways. Dust transport has been widely observed across continents, countries, provinces, and cities (Dey et al. 2004; Hegde et al. 2007; Gautam et al. 2009a; Christopher et al. 2011; Cao et al. 2014; Singh 2014; Athanasopoulou et al. 2016; Diaz-Hernandez and Sanchez-Navas 2016; Koo et al. 2016). In many cases, dust storms originate from the soils of arid and semiarid regions of the world, mainly from the desert regions (Prospero et al. 2002; Rashki et al. 2013). Dust originates from the northwestern China and the southern Mongolia (Zhang et al. 2003) that are transported for long distances, reaching vast areas in eastern China, Korea, Japan, cross over the Pacific ocean, and reach up to the western parts of the North America (Fairlie et al. 2007; Singh et al. 2008; Uno et al. 2011; Huang et al. 2012; Tong et al. 2012; Kaskaoutis et al. 2014; Tsai et al. 2014; Chen et al. 2015). In some areas, the limited rainfall with climate change leads to the wind erosion that produces dust affecting weather, meteorological, atmospheric, and air quality at local, regional, and global scale (Prasad and Singh 2007a, b; Prasad et al. 2007; Goudie 2009; Gautam et al. 2009b, c; Pokharel and Kaplan 2017). Dust contains fine particles, a serious health threat to the people living in the dust affected areas (Sprigg et al. 2014), and also impacts the ocean ecology (Singh et al. 2008) and radiation budget (Dey et al. 2004; Prasad and Singh 2007b; Gautam et al. 2009a; Raman et al. 2011; Chatterjee et al. 2012; Singh 2014; Kumar et al. 2015) that have long-term climate impacts. The dust storm events are observed frequently in India, China, Africa, Australia, Middle East region, and also over US continent almost every

✉ Ramesh P. Singh
rsingh@chapman.edu

1 School of Engineering and Technology, Sharda University, Knowledge Park III, Greater Noida 201306, India

2 School of Life and Environmental Sciences, Schmid College of Science and Technology, Chapman University, One University Drive, Orange, CA 92866, USA

3 Graduate Program in Cartographic Sciences, Department of Cartography, São Paulo State University (UNESP), Presidente Prudente, SP 19060-900, Brazil

year. The physical and chemical properties of dust vary from place to place, proximity to the ocean and these particles interact with the anthropogenic emissions and clouds, thus strong aerosol mixing is observed along the track of dust storms (Kaskaoutis et al. 2012). Enhancement in atmospheric water vapor and trace gases was observed during dust storm events in India and China (Bhattacharjee et al. 2007; Yoon et al. 2006; Cao et al. 2014). If the dust reaches to the higher elevation, the albedo of the snow/glaciers is severely affected. Snow/glaciers are darkened due to dust storms, absorbing more radiations that accelerate the melting of snow and glaciers (Prospero 1999; Tong et al. 2012; Painter et al. 2007; Prasad and Singh 2007b; Gautam et al. 2013; Cao et al. 2014; Singh 2014). Frequent dust events in Africa, China, Australia, Middle East, and India impact the air quality, atmosphere, climate, biogeochemical, ecological and meteorological parameters, radiative forcing, and earth system processes for short and long periods (Goudie 2009; Shao et al. 2011; Nastos 2012; Singh 2014; Cao et al. 2014; Parolari et al. 2016). Dust characteristics are extensively studied in different parts of the world (Eck et al. 1999; Gautam et al. 2013). In the North American region, a warmer and drier southwest USA (Seager 2007; Wu and Lau 2016; Zhou et al. 2016; Pokharel and Kaplan 2017), leading to increased wildfire risks and occurrence of dust storms (Westerling and Bryant 2008; Dennison et al. 2014).

In this paper, we have carried out detailed analysis of ground and satellite data and studied several aerosol optical (Aerosol Optical Depth—AOD, Ångström exponent, fine particles, single scattering albedo-SSA), air quality ($PM_{2.5}$, air quality index—AQI), trace gases (Nitrogen Dioxide—NO_2, Carbon monoxide—CO, Ozone—O_3), and meteorological parameters (relative humidity—RH, Temperature, Wind Speed and Direction, Pressure) associated with the dust event of September 28, 2016, which was observed over the city Bakersfield and its surroundings, California (USA). The results show pronounced mixing of dust and smoke from the forest fires, on the air quality index, air pollutants (CO, NO_2, and O_3). Such changes have direct impact on the weather conditions, visibility, meteorological parameters, and trace gas concentrations.

Dust event of September 28, 2016, and ground data related to meteorological parameters

Figure 1a shows the location of Bakersfield and surrounding areas, and the Mojave Desert lies in the east of Bakersfield. According to National Weather Service in Hanford (USA), dust outburst was seen during thunderstorm in and around Bakersfield, CA (USA) (Fig. 1b) on September 28, 2016, around 4.00 pm.

The AQI and meteorological data considered in this paper are obtained from the Air Resource Board of California Environmental Protection Board (ARB of CalEPB) (https://www.arb.ca.gov/homepage.htm). AQI simplifies the concentrations of several air pollutants for conventional monitor to single digit mode and characterizes air pollution level and air quality status. We have analyzed separately four air pollutants: nitrogen oxides (NO_2), carbon monoxide (CO), ozone (O_3), and air quality (particulate matter, $PM_{2.5}$) to study the effect of dust storm in Bakersfield, California. We have chosen two separate sites of ground monitoring, Bakersfield Municipal Airport (35.33°N, 119.00°W) and Bakersfield-5558 California Avenue (35.36°N, 119.06°W) for daily data retrieval. Daily averaged wind speed is also analyzed for these two sites. Rainfall data over Bakersfield are taken from US climate data (http://www.usclimatedata.com/climate/bakersfield/california/united-states/usca0062).

Due to dust storm, visibility was reduced to half km or less (http://www.turnto23.com/news/local-news/thunderstorm-rolls-into-bakersfield-wednesday). We have shown daily average wind speed, temperature, and pressure (Fig. 2a, b) at Bakersfield—5558 California Avenue (BK–CA) and Bakersfield Municipal Airport (BK–MA). Daily average wind speed on September 28, 2016, reaches to 29.61 km per hour at BK–MA and 15.12 km per hour at BK–CA (Fig. 2a). Temperature and pressure data are available only at BK–MA site along with wind speed. These are two air quality measurement sites of the Air Resource Board of California Environmental Protection Board. Prior to September 28, 2016, ambient temperature enhanced (Fig. 2b) with the low pressure caused formation of thunderstorm at Bakersfield followed by scattered unfrozen rainfall 0.27 kg per m^2. The area averaged rainfall (unfrozen) data have been obtained from NASA Giovanni website (https://giovanni.sci.gsfc.nasa.gov/giovanni/) with 0.125 degree resolution model data of the North American Land Data Assimilation System.

Strong wind speed up to 31.68 km per hour was observed with dominant southeast wind component brought the dust mass from the Mojave Desert (Fig. 3). Due to dust storm, visibility reduced to 2.8 km from the normal visibility up to 16 km and gust speed varies in the range 37–50 km/hr (Fig. 4). These data are taken from Bakersfield ground station (35.35°N, 118.97°W) (https://www.wunderground.com/US/CA/Bakersfield.html). The NOAA HYSPLIT trajectory model (http://ready.arl.noaa.gov/HYSPLIT.php) is used to track dust source at different altitudes. The back trajectories available after running NOAA HYSPLIT model are overlaid with the Google Earth and the images are analyzed. To compute the back trajectories, we have used meteorological data available from global data assimilation system (GDAS) developed by the global forecast system (GFS) model with spatial resolution of 1°. Figure 5 represents the NOAA HYSPLIT model back Trajectory with starting time 23 h

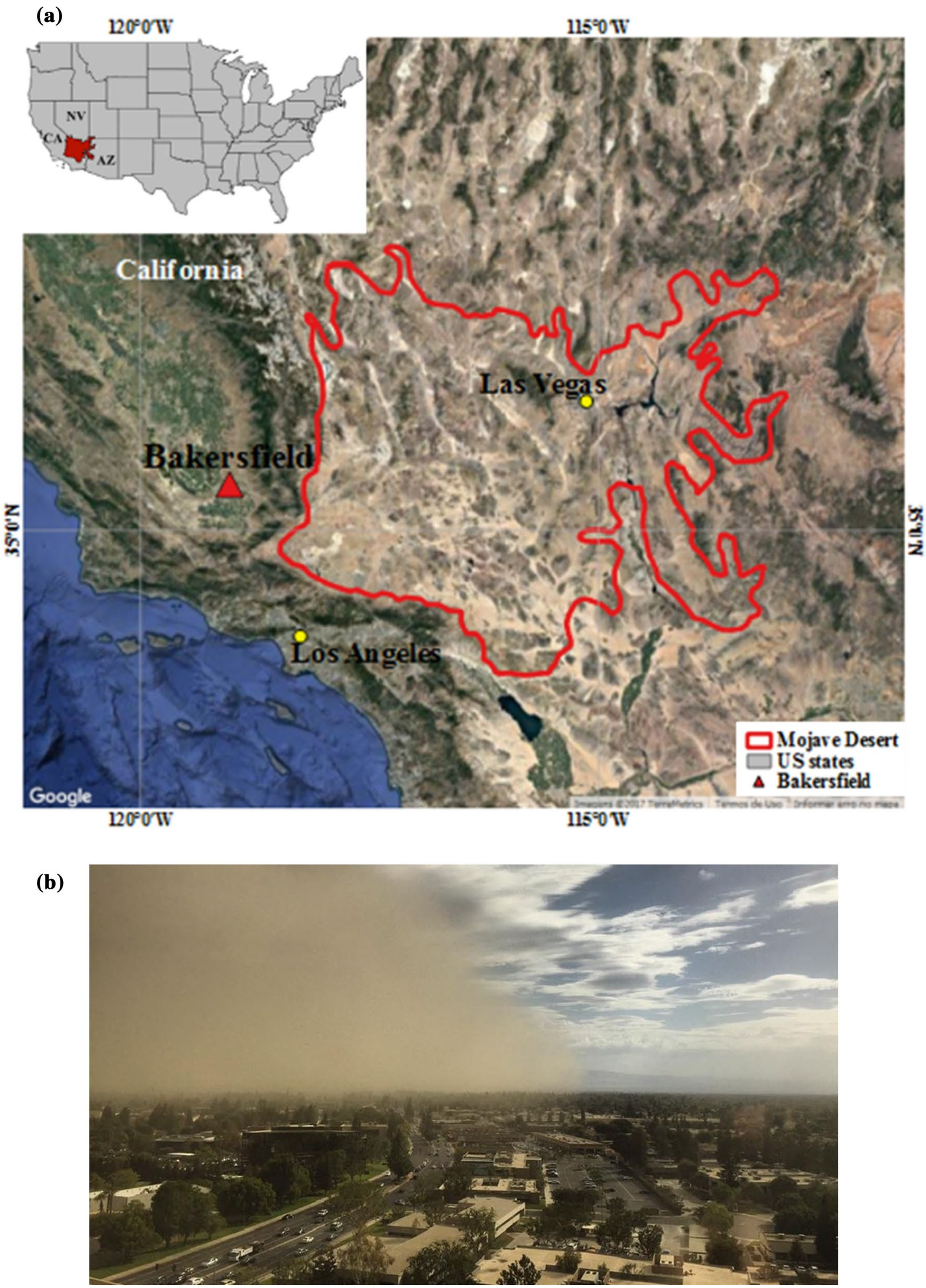

Fig. 1 **a** Google Earth image showing Bakersfield, California State boundary and Mojave Desert, **b** dust blowing into Bakersfield, CA (USA) on September 28, 2016, during thunderstorm (http://www.turnto23.com/news/local-news/thunderstorm-rolls-into-bakersfield-wednesday)

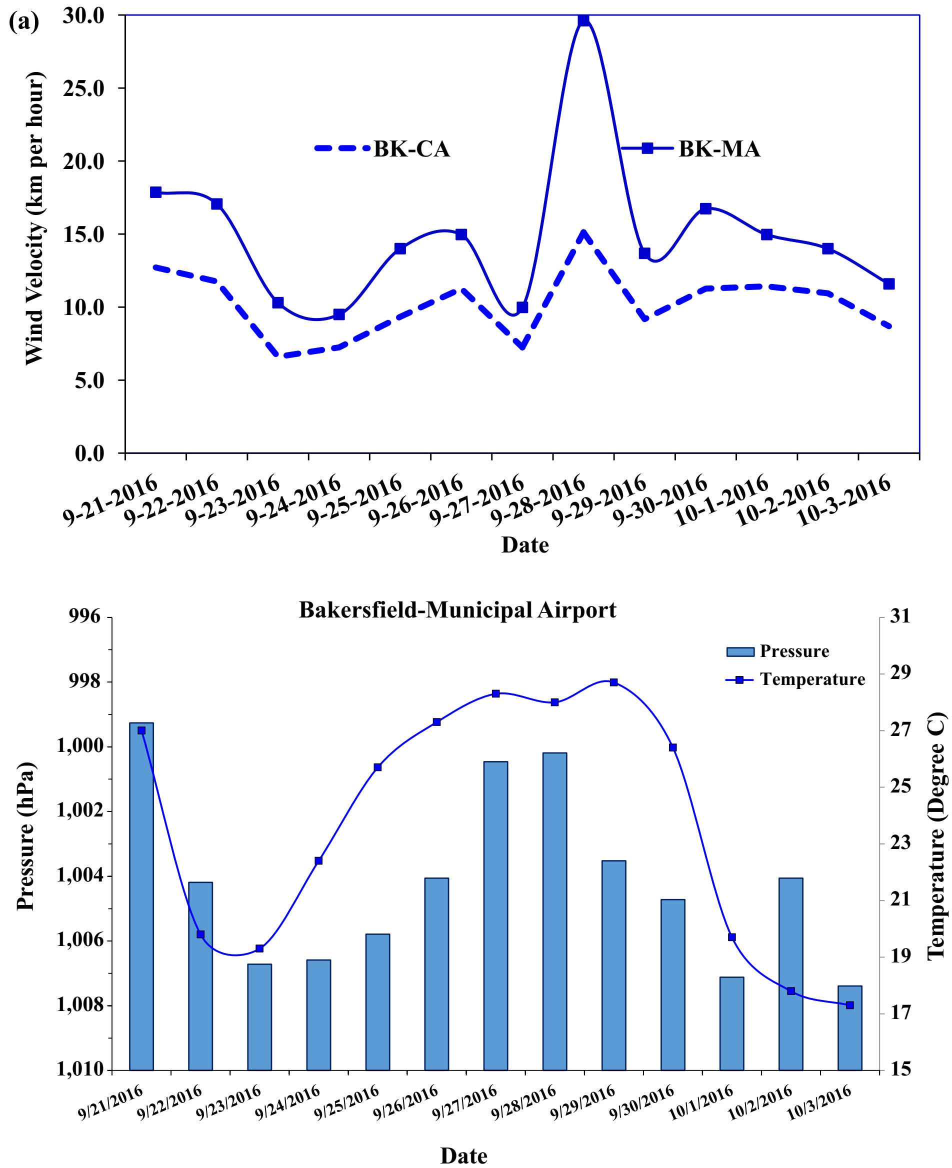

Fig. 2 **a** Daily average wind speed during September 21–October 3, 2016, at two locations Bakersfield–5558 California Avenue (BK–CA) and Bakersfield Municipal Airport (BK–MA), **b** daily average atmospheric pressure and surface temperature during September 21–October 3, 2016

on September 28, 2016. The back trajectory of airmass confirms that the source of dust storm observed in Bakersfield from the Mojave Desert located in the eastern parts of the Bakersfield.

Details of data used in the present study

AERONET and satellite data

Using AERONET data (Holben et al. 1998), changes in aerosol characteristics associated with the dust storms over the Indo-Gangetic basin and also in China have been studied (Prasad et al. 2007; Cao et al. 2014; Chauhan et al. 2016). We have used AERONET (version 2, Level 1.5, L1.5 is preliminary data) data from Bakersfield (35.33°N, 119.00°W). We have studied total column aerosols properties such as volume particle size distribution (dV/dLnR), refractive index, and single scattering albedo from this station during dusty and non-dusty days. The detailed methodology of retrieval of aerosol parameters from AERONET stations is discussed in detail by Dubovik and King (2000) and Dubovik et al. (2000). Further, we have used satellite-derived aerosol optical depth (AOD) and Ångström exponent (α) data (Collection 6) obtained from the moderate-resolution imaging spectroradiometer (MODIS) AQUA and TERRA satellites for the bounding area (34–35°N, 118–119°W) through the NASA Giovanni portal. NLDAS–Noah Land Surface Model L4 (hourly, 0.125 × 0.125 degree and version 2) rainfall (unfrozen) data have been used to study after effect of dust storm. We have used hourly meteorological data from Bakersfield ground station (35.35°N, 118.97°W) (https://www.wunderground.com/US/CA/Bakersfield.html) of wind speed and wind direction of the day September 28, 2016, were used to make

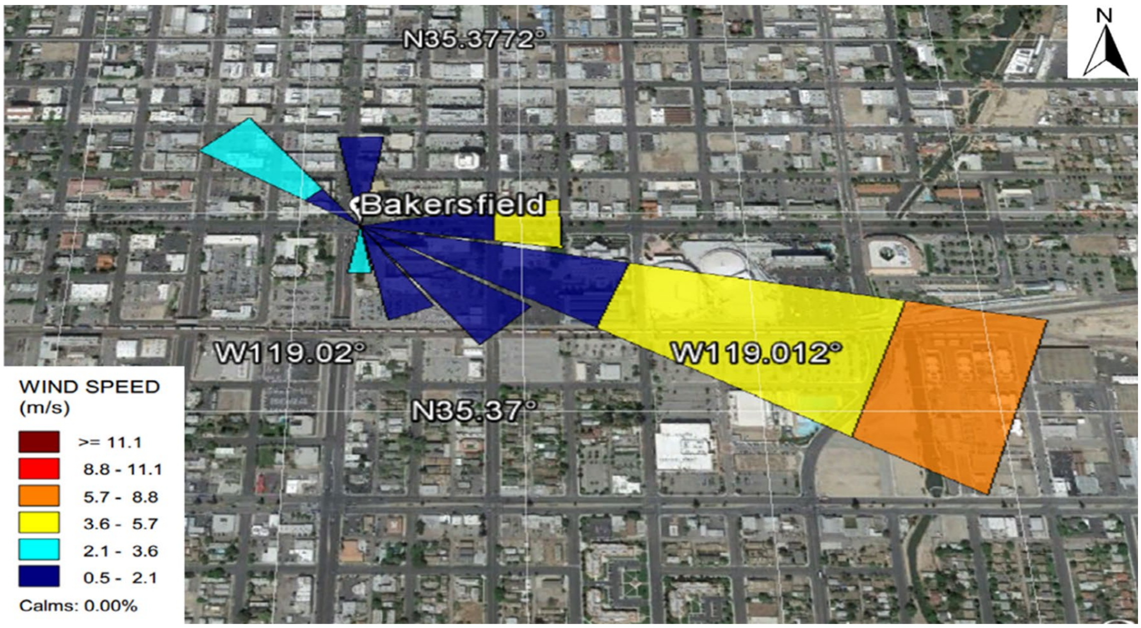

Fig. 3 Wind rose diagram for September 28 using meteorological data from Bakersfield monitoring station which is overlaid on Google Earth, southeast wind show a dominant component

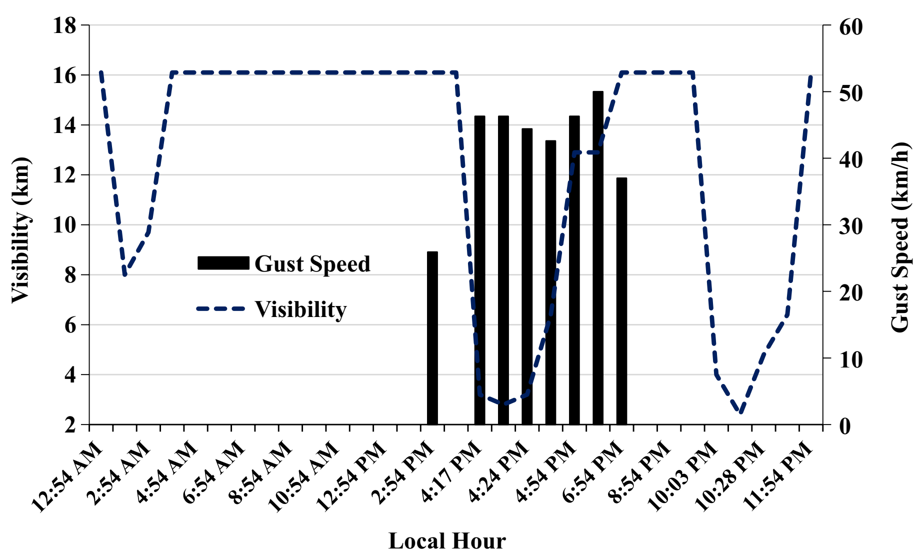

Fig. 4 Ground measurement of visibility and gust speed showing the influence of dust storm in and around Bakersfield on September 28, 2016

wind rose plot (WRPLOT Wind Rose Plots for Meteorology, version 7.0.0, (http://www.weblakes.com/products/wrplot/index.html) and analyze wind conditions.

Result and discussion

Variability of AOD and Ångström exponent from AERONET station

Figure 6 shows daily variations of aerosol optical depth (AOD) and Ångström exponent around Bakersfield. On an average AOD in the surroundings of Bakersfield was lower in general, average AOD (0.19) and AE of 0.66 were observed during September–October 01, 2016, from the Aqua MODIS and average AOD (0.18) and Ångström exponent (0.57) for the Terra MODIS during the same period.

Variations in the two data sets were due to different time of measurements but the variation was almost similar in both Terra and Aqua MODIS data. Dust event occurred in the evening around 4:00 pm on September 28, 2016, and satellite pass time over Bakersfield region was before 4:00 pm, so the effect of dust storm was not seen on September 28, 2016. Pronounced effect of dust storm was clearly seen on

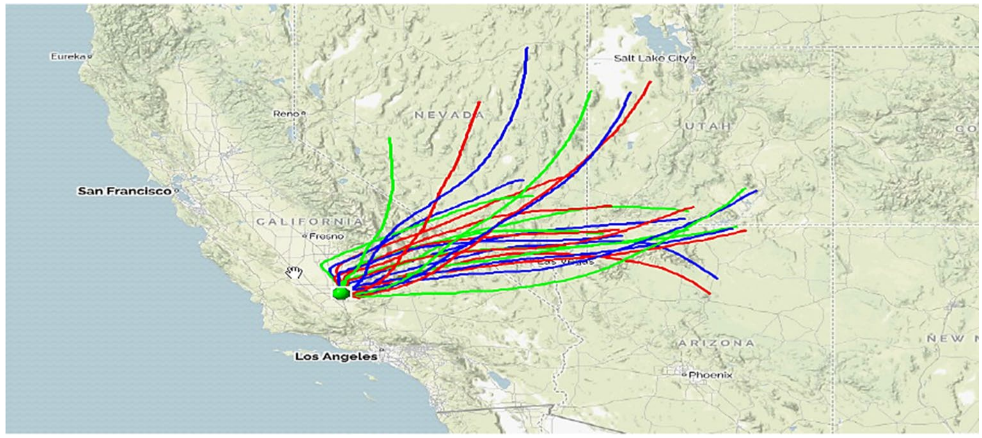

Fig. 5 Shows NOAA back trajectories on October 1, 2016, the airmass reaching over Bakersfield within 24 h at altitudes 500 m, different color trajectories show change in the airmass reaching in Bakersfield within 24 h, and the dominant airmass is from the Mojave Desert located in the eastern side of Bakersfield

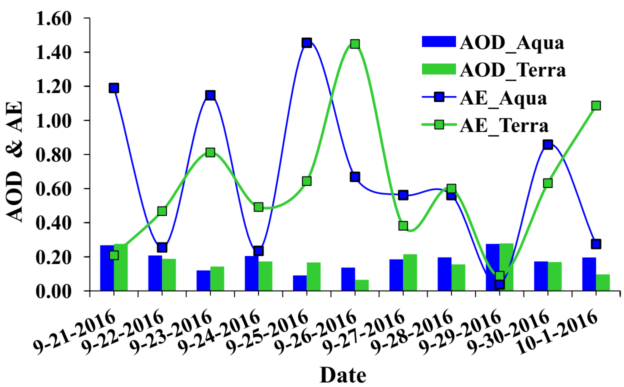

Fig. 6 Daily variations of AOD and AE (MODIS data)

the next day September 29, 2016. On September 28, 2016, low AOD (0.20 and 0.16) with high Ångström exponent (0.56 and 0.60) was observed prior to the dust storm. Higher Ångström exponent clearly shows the presence of fine particles from the forest fires and also anthropogenic activities. On September 29, 2016, after dust storm AOD was high (0.28) with low Ångström exponent (0.04 and 0.09), showing characteristics of dust. Low AE values are the characteristics of coarse particles due to dust. Dust event occurred on September 28, 2016, and the effect was clearly evident on the next day, showing the presence of course particles for long period in the atmosphere.

Changes in air quality parameters

We have considered average daily data from two ground monitoring stations. The daily average of all AQI parameters (CO, $PM_{2.5}$, NO_2, NO_x, and O_3) is shown for the period 21 September 21, 2016–October 03, 2016, in Fig. 7a–c. Prior to September 28, 2016, the wind speed in Bakersfield was low, but high CO (0.28 ppm) and $PM_{2.5}$ (18 µgm/m^3) were observed (Fig. 7a). CO is the main sources from vehicular emissions and forest fire, and higher CO (Fig. 7a) is likely from the emissions from forest fires on September 23–27 northwest of Bakersfield area. The back trajectories (Fig. 5) confirm that the airmass reaching at the Bakersfield coming from the ongoing forest fire, that may enhance CO concentrations which is obvious. In general, during winter season, $PM_{2.5}$ concentrations reach up to 50 µgm/m^3 which was recently reported by Nallathamby et al. (2014). In the afternoon on September 28, 2016, the wind was strong and dust storm occurred in Bakersfield area, a sharp sudden drop in CO (0.21 ppm) and increase in $PM_{2.5}$ (19 µgm/m^3) was observed. On September 29, 2016, due to strong aerosol mixing, sudden drop in CO (0.18 ppm) and $PM_{2.5}$ (12.80 µgm/m^3) was observed (Fig. 7a).

Figure 7b shows changes in surface ozone (O_3) on the dusty days from the two sites of ARB located at Bakersfield (BK–MA and BK–CA). The average ozone during September 21, 2016–October 03, 2016, was about 0.036 and 0.035 ppm, respectively, at BK–MA and BK–CA sites. Prior to the dust event, i.e., on September 27, 2106, Ozone concentration was 0.042 and 0.04 ppm at the two locations, after the dust storm the concentrations were decreased on September 28, 2016, up to 0.032 and 0.033 ppm at two locations. On September 29, 2016, Ozone concentrations (0.035 and 0.036 ppm, respectively, at BK–MA and BK–CA) increased but it was still low 0.041 at both the stations on September 30, 2016, this is obvious due to forest fire plume reaching in Bakersfield. Similar results are also observed during desert dust by Eck et al. (1999) and O'Neill et al. (2001). After the dust storm, an enhancement in Ozone concentration was observed (Fig. 7b) which could be due to advection from the troposphere to stratosphere. Due to the forest fire, an enhancement in NO_2 was observed till September 27, 2016, showing the effect of forest fire in Bakersfield region, however, the NO_2 and NO_x concentrations decreased during and after the dust event (Fig. 7c).

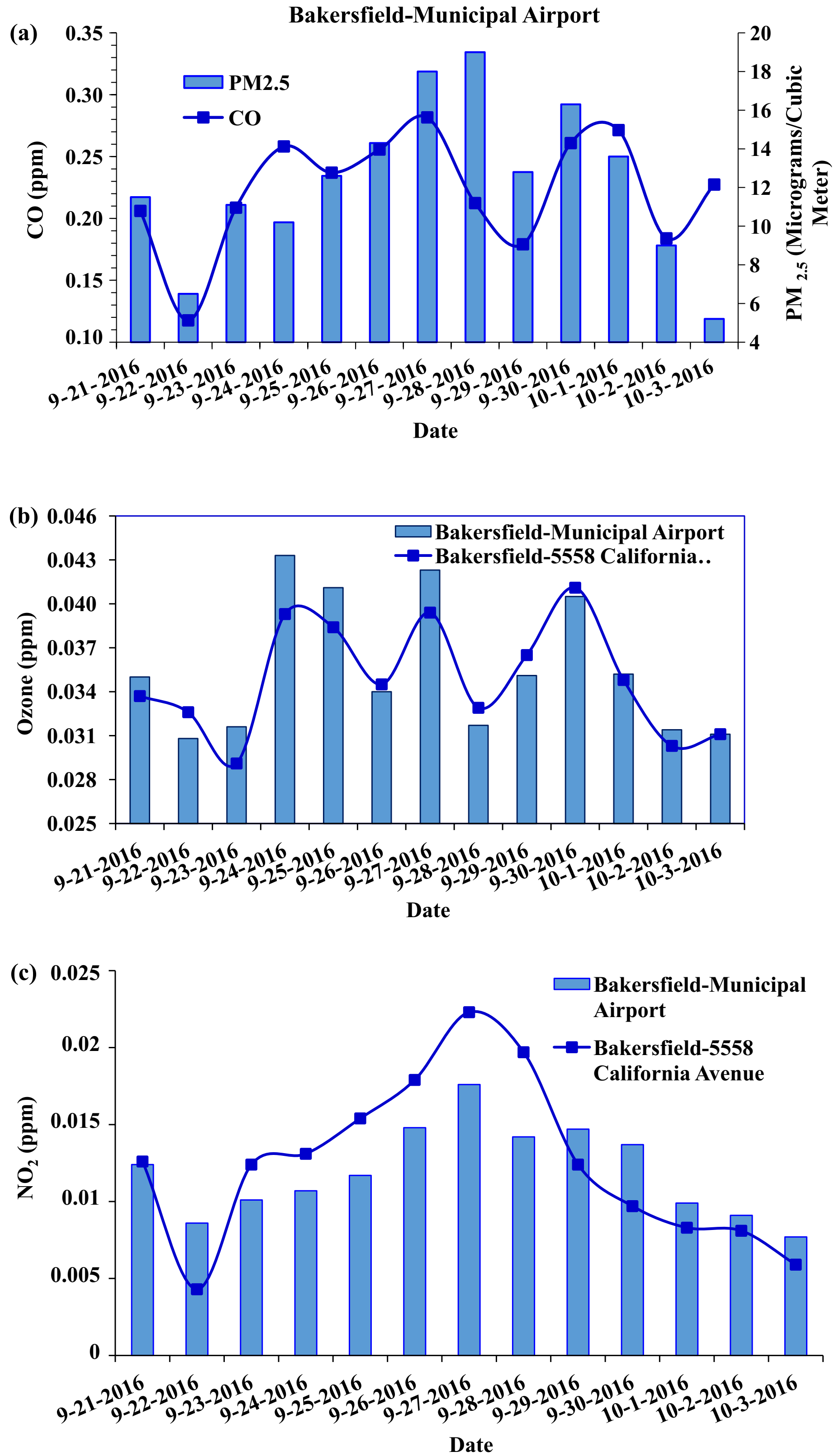

Fig. 7 **a** Daily variation of CO and $PM_{2.5}$, **b** daily variation ozone (ppm), **c** daily variation of NO_2 (ppm) during September 21–October 3, 2016

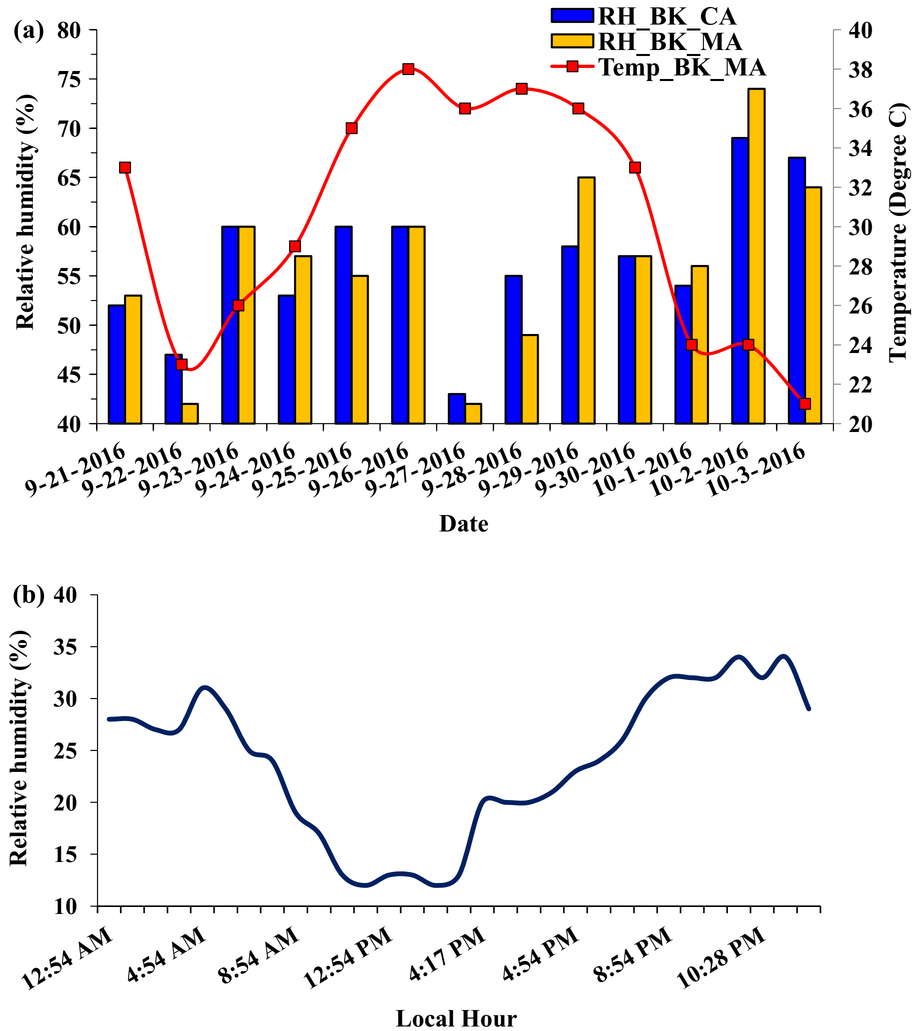

Fig. 8 **a** Daily variation of relative humidity and temperature during September 21–October 3, 2016, **b** ground observed relative humidity shows enhancement in relative humidity associated with the dust event in Bakersfield observed at around 4 pm on September 28, 2016

Changes in relative humidity and air temperature

Figure 8a shows daily relative humidity (%) and day maximum temperature (°C) over the two sites of ARB located at Bakersfield (BK–MA and BK–CA). Temperature data were available only at BK–MA location. During September 21, 2016–October 3, 2016, average daily relative humidity was 56.54 and 56.46%, respectively, at BK–CA and BK–MA locations and average temperature were found to be around 30.38 °C at BK–MA location. Prior to the dust event, relative humidity declines to 43% over BK–CA and 42% over BK–MA, a slight decrease in temperature (36 °C) well above the average value was observed. On the dust day, relative humidity increased (55% over BK–MA and 49% over BK–CA), showing that the site BK–MA was more affected by dust storm, and sharp enhancement up to 86% in RH was observed with a drop in temperature on September 29, 2016. A sharp reduction in the relative humidity associated with the dust storm was observed from the ground weather station located in Bakersfield. The increased temperature leads to an increase in the saturated vapor pressure point. In this case, the water vapor in the air becomes more difficult to coagulate (Hu et al. 2017). After the dust storm, relative humidity steadily increased and reached at the maximum level (about 35%) after 8 pm local time.

Fig. 9 **a** Particle size distribution, **b** variations of single scattering albedo (SSA) during September 25–October 9, 2016, **c** showing forward trajectories computed using NOAA HYSPILT model (https://ready.arl.noaa.gov/HYSPLIT_traj.php) from forest fire in Santa Cruz mountain (latitude 37 N and longitude 121.4 W) showing airmass reaching to Bakersfield (located in southeast), the airmass from forest fires mixed with the dust storm observed in Bakersfield on 28 September 2016

Changes in volume density and particle size

Figure 9a shows an increase in the volume density of large particles derived from Bakersfield AERONET station soon after the dust event on September 29 until October 1, 2016, afterward concentrations of large particles decreased. In

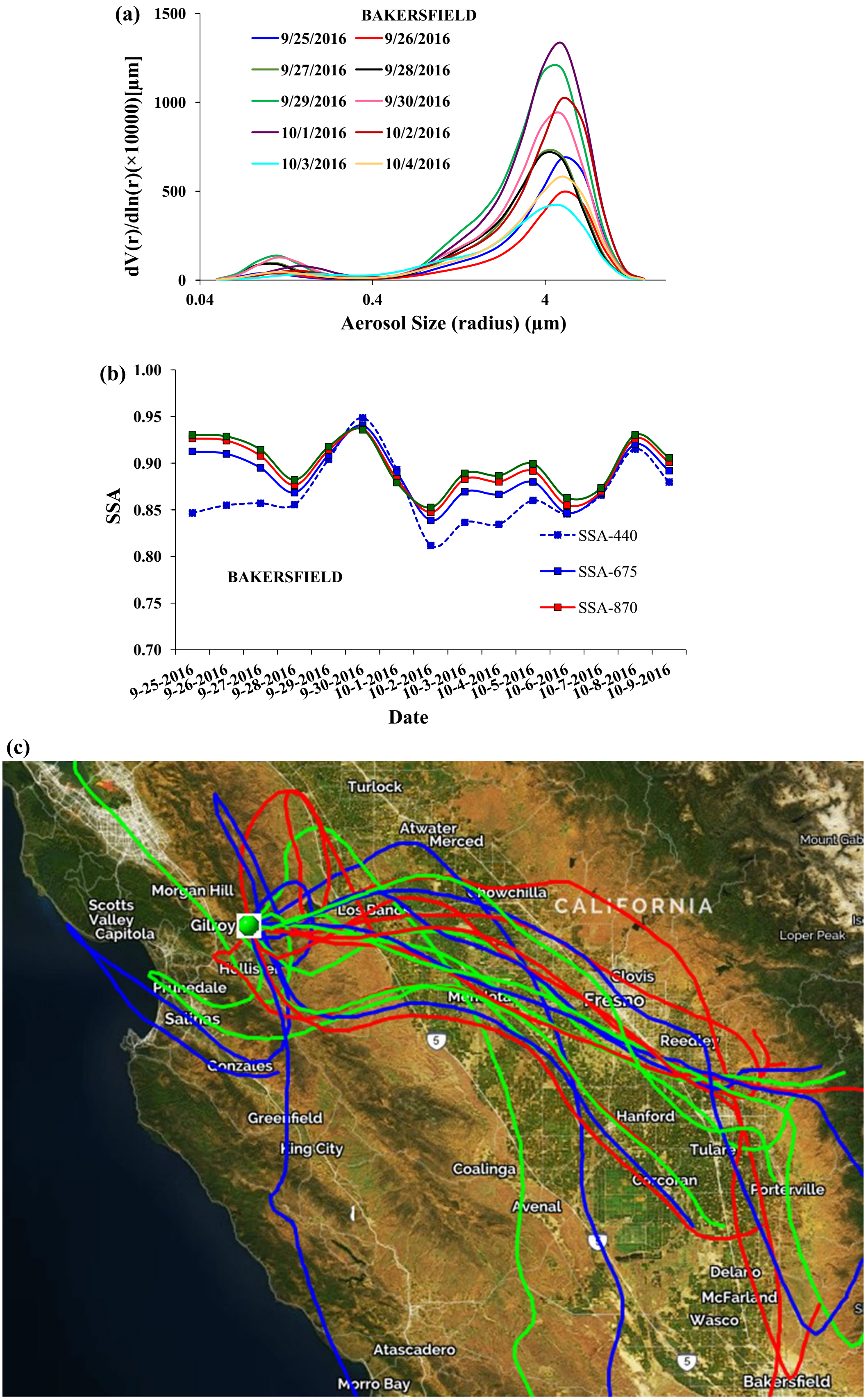
(a)
BAKERSFIELD
9/25/2016
9/26/2016
9/27/2016
9/28/2016
9/29/2016
9/30/2016
10/1/2016
10/2/2016
10/3/2016
10/4/2016
dV(r)/dln(r)(×10000)[µm]
1500
1000
500
0
0.04
0.4
4
Aerosol Size (radius) (µm)
(b)
1.00
0.95
0.90
0.85
0.80
0.75
0.70
SSA
BAKERSFIELD
SSA-440
SSA-675
SSA-870
9-25-2016
9-26-2016
9-27-2016
9-28-2016
9-29-2016
9-30-2016
10-1-2016
10-2-2016
10-3-2016
10-4-2016
10-5-2016
10-6-2016
10-7-2016
10-8-2016
10-9-2016
Date
(c)
Turlock
Atwater
Merced
Morgan Hill
Scotts Valley
Capitola
Gilroy
Los Banos
CALIFORNIA
Loper Peak
Clovis
Fresno
Salinas
Reedley
Hanford
Greenfield
King City
Tulare
Coalinga
Corcoran
Porterville
Avenal
Delano
McFarland
Wasco
Atascadero
Morro Bay
Bakersfield

surrounding areas of Bakersfield, forest fire occurred in northwest location during September 17–24 at Canyon, Santa Barbara County, consequently SSA decreased during September 25–28 showing increasing concentrations of black carbon. A strong mixing of dust and black carbon from the forest fire on September 28, 2016, was clearly reflected from the increase in SSA values and also due to strong wavelength contrast in the absence of dust event (Fig. 9b). The strong wavelength dependency of SSA especially with low SSA clearly shows dominance of black carbon particles due to mixing of dust aerosols and plume from forest fires. The NOAA forward trajectories (Fig. 9c) clearly show transport of airmass (emissions) reaching to Bakersfield that have mixed with the black carbon particles in the atmosphere of Bakersfield and surroundings.

Conclusion

California State is adjacent to the Mojave Desert in the east, and forest fire is very common during spring and summer especially when Santa Ana winds are prevalent. Santa Ana winds are characterized by strong winds, low humidity, and higher temperature originated from Mojave Desert located adjacent to California in the eastern part. During Santa Ana winds, easterly and north-easterly winds bring airmass containing dust particles from dust, as a result the air quality degraded, visibility reduced, and weather conditions change drastically. Detailed analysis of the ground and satellite data shows pronounced changes in air quality, trace gases, meteorological and aerosol optical parameters, and also changes in aerosol optical parameters associated with September 28, 2016, dust storm. The volume density of large size aerosol particles enhanced due to dust event. Prior to the dust event, forest fire occurred in the surrounding areas showing enhancement in CO, and NO_2 concentrations, but the ozone concentrations of the ground level reduced. The SSA retrieved from Bakersfield AERONET station, characterized by low and high SSA, low SSA is characterized by the presence of absorbing aerosols (carbon soot) in the atmosphere (i.e., likely to be associated with the forest fire. The NOAA back trajectories clearly show arrival of dust mass from desert region that have mixed with the smoke plume containing black carbon particles (higher SSA values) from the northwest forest fire. In California, forest fire frequently occurs every year, during this period dust from the adjacent Mojave Desert area are likely to mix that will influence atmospheric chemistry and weather conditions. Quantitative evaluation of mixing and its impact on atmospheric and meteorological parameters will help the atmospheric and climate community for better forecast of weather conditions.

Acknowledgements The authors thank the California Environmental Protection Board and meteorological station, AERONET and NASA Giovanni and NOAA HYSPLIT teams for freely providing different data sets which was used in the present study. One of the authors (Samara Calçado de Azevedo) is thankful to FAPESP (2015/26743-5) for the award fellowship to visit Chapman University, she is also grateful to Daniele Struppa, President, Chapman University for his permission to use facilities and library resources. The authors are grateful to two anonymous reviewers for their comments/suggestions that have helped us to improve earlier version of the manuscript.

References

Athanasopoulou E, Protonotariou A, Papangelis G, Tombrou M, Mihalopoulos N, Gerasopoulos E (2016) Long-range transport of Saharan dust and chemical transformations over the Eastern Mediterranean. Atmos Environ 140:592–604. https://doi.org/10.1016/j.atmosenv.2016.06.041

Bhattacharjee PS, Prasad AK, Kafatos M, Singh RP (2007) Influence of a dust storm on carbon monoxide and water vapor over the Indo-Gangetic Plains. J Geophys Res 112:D18203. https://doi.org/10.1029/2007JD008469

Cao CX, Zheng S, Singh RP (2014) Characteristics of aerosol optical properties and meteorological parameters during three major dust events (2005–2010) over Beijing, China. Atmos Res 150:129–142

Chatterjee A, Ghosh SK, Adak A, Singh AK, Devara PCS, Raha S (2012) Effect of dust and anthropogenic aerosols on columnar aerosol optical properties over Darjeeling (2200 m asl), Eastern Himalayas, India. PLoS ONE 7(7):e40286. https://doi.org/10.1371/journal.pone.0040286

Chauhan A, Zheng S, Xu M, Cao C, Singh RP (2016) Characteristic changes in aerosol and meteorological parameters associated with dust event of 9 March 2013. Model Earth Syst Environ 2:181. https://doi.org/10.1007/s40808-016-0236-1

Chen Y, Luo B, Xie SD (2015) Characteristics of the long-range transport dust events in Chengdu, Southwest. Atmos Environ 122:713–722. https://doi.org/10.1016/j.atmosenv.2015.10.045

Christopher SA, Gupta P, Johnson B, Ansell C, Brindley H, Haywood J (2011) Multi-sensor satellite remote sensing of dust aerosols over North Africa during GERBILS. Q J R Meteorol Soc 137:1168–1178

Dennison PE, Brewer SC, Arnold JD, Moritz MA (2014) Large wildfire trends in the western United States, 1984–2011. Geophys Res Lett 41:2928–2933. https://doi.org/10.1002/2014GL059576

Dey S, Tripathi SN, Singh RP, Holben BN (2004) Influence of dust storms on aerosol optical properties over the Indo-Gangetic basin. J Geophys Res 109:D20211. https://doi.org/10.1029/2004JD004924

Diaz-Hernandez JL, SanchezNavas A (2016) Saharan dust outbreaks and iberulite episodes. J Geophys Res Atmos 121:7064–7078. https://doi.org/10.1002/2016JD024913

Dubovik O, King MD (2000) A flexible inversion algorithm for retrieval of aerosol optical properties from Sun and sky radiance measurements. J Geophys Res 105:20673–20696

Dubovik O, Holben BN, King MD, Kaufman YJ, Smirnov A, Eck TF, Slutsker I (2000) Accuracy assessments of aerosol optical properties retrieved from AERONET Sun and sky-radiance measurements. J Geophys Res 105:9791–9806

Eck TF, Holben BN, Reid JS, Dubovik O, Smironov A, O'Neill NT, Slutsker I, Kinne S (1999) Wavelength dependence of the optical depth of biomass burning, urban, and desert dust aerosol. J Geophys Res 104:31333–31350

Fairlie TD, Jacob DJ, Park RJ (2007) The impact of transpacific transport of mineral dust in the United States. Atmos Environ 41:1251–1266

Gautam R, Liu ZY, Singh RP, Hsu NC (2009a) Two contrasting dust-dominant periods over India observed from MODIS and CALIPSO data. Geophy Res Lett 36:L06813. https://doi.org/10.1029/2008GL036967

Gautam R, Hsu NC, Lau K-M, Tsay S-C, Kafatos M (2009b) Enhanced pre-monsoon warming over the Himalayan–Gangetic region from 1979 to 2007. Geophys Res Lett 36:L07704. https://doi.org/10.1029/2009GL037641

Gautam R, Hsu NC, Lau K-M, Kafatos M (2009c) Aerosol and rainfall variability over the Indian monsoon region: distributions, trends and coupling. Ann Geophys 27:3691–3703. https://doi.org/10.5194/angeo-27-3691-2009

Gautam R, Hsu NC, Lau K-M, Yasunari TJ (2013) Satellite observations of desert dust-induced Himalayan snow darkening. Geophys Res Lett 40:988–993. https://doi.org/10.1002/grl.50226

Goudie AS (2009) Dust storms: recent developments. J Environ Manage 90:89–94. https://doi.org/10.1016/j.jenvman.2008.07.007

Hegde P, Pant P, Naja M, Dumka UC, Sagar R (2007) South Asian dust episode in June 2006: aerosol observations in the central Himalayas. Geophys Res Lett 34:L23802. https://doi.org/10.1029/2007GL030692

Holben BN, Eck TF, Slutsker I, Tanré D, Buis JP, Setzer A, Vermote E, Reagan JA, Kaufman YJ, Nakajima T, Lavenu F, Jankowiak I, Smirnov A (1998) AERONET-A federated instrument network and data archive for aerosol characterization. Remote Sens Environ 66:1–16. https://doi.org/10.1016/S0034-4257(98)00031-5

Hu T, Wu D, Li Y, Wang C (2017) The effects of sandstorms on the climate of northwestern China. Adv Meteorol. https://doi.org/10.1155/2017/4035609

Huang K, Zhuang G, Lin Y, Fu JS, Wang Q, Liu T, Zhang R, Jiang Y, Deng C, Fu Q, Hsu NC, Cao B (2012) Typical types and formation mechanisms of haze in an Eastern Asia megacity, Shanghai. Atmos Chem Phys 12:105–124

Kaskaoutis DG, Gautam R, Singh RP, Houssos EE, Goto D, Singh S, Bartzokas A, Kosmopoulos PG, Sharma M, Hsu NC, Holben BN, Takmura T (2012) Influence of anomalous dry conditions on aerosols over India: transport, distribution and properties. J Geophys Res 117:D09106. https://doi.org/10.1029/2011JD017314

Kaskaoutis DG, Rashki A, Houssos EE, Mofidi A, Goto D, Bartzokas A, Francois P, Legrand M (2014) Meteorological aspects associated with dust storms in the Sistan region, southeastern Iran. Clim Dyn. https://doi.org/10.1007/s00382-014-2208-3

Koo JH, Kim J, Kim J, Lee H, Noh YM, Lee YG (2016) Springtime trans-pacific transport of asian pollutants characterized by the western pacific (WP) pattern. Atmos Environ 147:166–177. https://doi.org/10.1016/j.atmosenv.2016.10.007

Kumar S, Kumar S, Kaskaoutis DG, Singh RP, Singh RK, Mishra AK, Srivastava MK, Singh AK (2015) Meteorological, atmospheric and climatic perturbations during major dust storms over Indo-Gangetic Basin. Aeolian Res 17:15–31

Nallathamby PD, Lewandowski M, Jaoui M, Offenberg JH, Kleindienst TE, Rubitschun C, Surratt JD, Usenko S, Sheesley RJ (2014) Qualitative and quantitative assessment of unresolved complex mixture in $PM_{2.5}$ of Bakersfield, CA. Atmos Environ 98:368–375

Nastos PT (2012) Meteorological patterns associated with intense Saharan dust outbreaks over Greece in winter. Adv Meteorol. https://doi.org/10.1155/2012/828301

O'Neill NT, Eck TF, Holben BN, Smirnov A, Dubovik O, Royer A (2001) Bimodal size distribution influences on the variation of Angstrom derivatives in spectral and optical depth space. J Geophys Res 106:9787–9806

Painter TH, Barrett AP, Landry CC, Neff JC, Cassidy MP, Lawrence CR, McBride KE, Farmer GL (2007) Impact of disturbed desert soils on duration of mountain snow cover. Geophys Res Lett 34:L12502. https://doi.org/10.1029/2007GL030284

Parolari AJ, Li D, Bou-Zeid E, Katul GG, Assouline S (2016) Climate, not conflict, explains extreme middle east dust storm. Geophys. Res. Lett. 11(11):114013. https://doi.org/10.1088/1748-9326/11/11/114013

Pokharel AK, Kaplan ML (2017) Dust climatology of the NASA dryden flight research center (DFRC) in Lancaster, California, USA. Climate 5:15. https://doi.org/10.3390/cli5010015

Prasad AK, Singh RP (2007a) Changes in aerosol parameters during major dust storm events (2001–2005) over the Indo-Gangetic Plains using AERONET and MODIS data. J Geophys Res 112:D09208. https://doi.org/10.1029/2006JD007778

Prasad AK, Singh RP (2007b) Changes in Himalayan snow and glacier cover between 1972 and 2000. EOS Trans AGU 88:326. https://doi.org/10.1029/2007EO330002

Prasad AK, Singh S, Chauhan SS, Srivastava MK, Singh RP, Singh R (2007) Aerosol radiative forcing over the Indo-Gangetic plains during major dust storms. Atmos Environ 41:6289–6301

Prospero JM (1999) Long-term measurements of the transport of African mineral dust to the southeastern United States: implications for regional air quality. J Geophys Res 104:15917–15927

Prospero JM, Ginoux P, Torres O, Nicholson SE (2002) Environmental characterization of global sources of atmospheric soil dust derived from the NIMBUS-7 TOMS absorbing aerosol product. Rev Geophys 40(1):1002. https://doi.org/10.1029/20000GR000095

Raman RS, Ramachandran S, Kedia S (2011) A methodology to estimate source-specific aerosol radiative forcing. J Aerosol Sci 42(5):305–320. https://doi.org/10.1016/j.jaerosci.2011.01.008

Rashki A, Kaskaoutis DG, Goudie AS, Kahn RA (2013) Dryness of ephemeral lakes and consequences for dust activity: the case of the Hamoun drainage basin, southeastern Iran. Sci Total Environ 463:552–564

Seager R (2007) The turn of the century North American drought: global context, dynamics, and past analogs. J Clim 20:5527–5552

Shao Y, Wyrwoll KH, Chappell A, Huang J, Lin Z, McTainsh GH, Mikami M, Tanaka TY, Wangh X, Yoon S (2011) Dust cycle: an emerging core theme in Earth system science. Aeolian Res 2:181–204

Singh RP (2014) Dust storms and their influence on atmospheric parameters over the Indo-Gangetic plains, book chapter 2. In: Sundaresan J et al (eds) Geospatial technologies and climate change, vol 10. Springer, Cham, pp 21–35. https://doi.org/10.1007/978-3-319-01689-4_2

Singh RP, Prasad AK, Kayetha VK, Kafatos M (2008) Enhancement of oceanic parameters associated with dust storms using satellite data. J Geophys Res 113:C11008. https://doi.org/10.1029/2008JC004815

Sprigg WA, Nickovic S, Galgiani JN, Pejanovic G, Petkovic S, Vujadinovic M, Vukovic A, Dacic M, DiBiase S, Prasad A, El-Askary H (2014) Regional dust storm modeling for health services: the case of valley fever. Aeolian Res 14:53–73

Tong DQ, Dan M, Wang T, Lee P (2012) Long term dust climatology in the western United States reconstructed from routine aerosol ground monitoring. Atmos Chem Phys 12:5189–5205. https://doi.org/10.5194/acp-12-5189-2012

Tsai F, Tu J-Y, Hsu S-C, Chen W-N (2014) Case study of the Asian dust and pollutant event in spring 2006: source, transport, and contribution to Taiwan. Sci Total Environ 478:163–174

Uno I, Eguchi K, Yumimoto K, Liu Z, Hara Y, Sugimoto N, Shimizu A, Takemura T (2011) Large Asian dust layers continuously reached North America in April 2010. Atmo Chem Phys 11:7333–7341

Westerling AL, Bryant BP (2008) Climate change and wildfire in California. Clim Change 87:S231–S249

Wu H-TJ, Lau WK-M (2016) Detecting climate signals in precipitation extremes from TRMM (1998–2013)—Increasing contrast between wet and dry extremes during the "global warming hiatus".

Geophys Res Lett 43:1340–1348. https://doi.org/10.1002/2015GL067371
Yoon S-C, Kim S-W, Kim J, Sohn B-J, Jefferson A, Choi S-J, Cha D-H, Weber RJ (2006) Enhanced water vapor in Asian dust layer: entrainment processes and implication for aerosol optical properties. Atmos Environ 40(13):2409–2421
Zhang XY, Gong SL, Shen ZX, Mei FM, Xi XX, Liu LC, Zhou ZJ, Wang D, Wang YQ, Cheng Y (2003) Characterization of soil dust aerosol in China and its transport and distribution during 2001 ACE-Asia: 1. Network observations. J Geophys Res Atmos. https://doi.org/10.1029/2002JD002632
Zhou Y, Wu D, Lau W, Tao WK (2016) Scale dependence of land-atmosphere interactions in wet and dry regions as simulated with NU-WRF over the southwestern and south-central United States. Hydrometeorology 17:2121–2136. https://doi.org/10.1175/JHM-D-16-0024.1